Optical clearing of the skin for near-infrared fluorescence image-guided surgery

Aya Matsui
Beth Israel Deaconess Medical Center
Department of Medicine
Division of Hematology/Oncology
Boston, Massachusetts 02215

Stephen J. Lomnes
GE Healthcare
Princeton, New Jersey 08540

John V. Frangioni
Beth Israel Deaconess Medical Center
Department of Medicine
Division of Hematology/Oncology
    and
Department of Radiology
Boston, Massachusetts 02215

Abstract. Near-infrared (NIR) light penetrates relatively deep into skin, but its usefulness for biomedical imaging is constrained by high scattering of living tissue. Previous studies have suggested that treatment with hyperosmotic "clearing" agents might change the optical properties of tissue, resulting in improved photon transport and reduced scatter. Since this would have a profound impact on image-guided surgery, we seek to quantify the magnitude of the optical clearing effect in living subjects. A custom NIR imaging system is used to perform sentinel lymph node mapping and superficial perforator angiography *in vivo* on 35-kg pigs in the presence or absence of glycerol or polypropylene glycol:polyethylene glycol (PPG:PEG) pretreatment of skin. *Ex-vivo*, NIR fluorescent standards are placed at a fixed distance beneath sections of excised porcine skin, either preserved in saline or stored dry, then treated or not treated with glycerol. Fluorescence intensity through the skin is quantified and analyzed statistically. Surprisingly, the expected increase in intensity is not measurable either *in vivo* or *ex vivo*, unless the skin is previously dried. Histological evaluation shows a morphological difference only in stratum corneum, with this difference being negligible in living tissue. In conclusion, topically applied hyperosmotic agents are ineffective for image-guided surgery of living subjects. © *2009 Society of Photo-Optical Instrumentation Engineers.* [DOI: 10.1117/1.3103317]

Keywords: optical clearing; hyperosmotic agents; near-infrared fluorescence; image-guided surgery.

Paper 08284RR received Aug. 12, 2008; revised manuscript received Jan. 20, 2009; accepted for publication Jan. 22, 2009; published online Apr. 3, 2009.

1 Introduction

Photon absorption and scatter in tissue limit the effectiveness of many optical techniques in biomedical imaging. Although near-infrared (NIR) wavelengths between 700 and 900 nm improve the signal-to-background ratio (SBR) by lowering absorption, scatter, and tissue autofluorescence (reviewed in Ref. 1), image-guided surgery, in particular, would benefit from improved photon transport.

In recent years, the optical clearing effects of hyperosmotic agents have generated great interest. Previous studies have shown that biological objects such as skin,[2] muscle,[3] gastric mucosa,[4] and dura mater[5] can be "cleared" with the application of hyperosmotic agents. Vargas et al.[6] suggested that hyperosmotic agents improve image contrast and depth capability, including scatter reduction, in two ways: 1. simple refractive index matching between hyperosmotic agents and tissue components, and 2. dehydration creating a refractive index matching environment with densely packed intracellular components. On the contrary, Yeh et al.[7] suggested that hyperosmotic agents induce structural modification or dissociation of collagen as their primary mechanism of action, a claim supported by studies showing a correlation between optical clearing and the agent's collagen solubility,[8] and studies showing a lack of correlation with either osmolality or refractive index.[9]

These three possible mechanisms of action are based on the premise that hyperosmotic agents can permeate far enough into tissue to alter optical properties. In fact, in most published studies, immersion or dermal side application was used to expose objects to hyperosmotic agents by avoiding the biological barrier of the stratum corneum (SC), the outermost layer of the skin. In studies on visceral organs, which have no SC, the direct application of hyperosmotic agents was suggested to cause inflammation, which in turn alters optical properties.[5,10] Although rehydration with isotonic saline may morphologically reverse undesirable irritation caused by direct application of active osmotic agents,[7,10,11] long-term functional reversibility has not been studied.

Thus, although optical clearing has been studied in several model systems, no definitive mechanism of action has been defined, and most model systems are not relevant to clinical translation of the technology. Our laboratory has previously applied NIR fluorescence imaging to skin sentinel lymph node (SLN) mapping[12] and superficial perforator angiography,[13] which targets superficial structures. Hyperosmotic agents could potentially enhance the imaging of these structures. In

Address all correspondence to: John V. Frangioni, M.D., Ph.D., BIDMC, Room SL-B05, 330 Brookline Avenue, Boston, MA 02215. Tel: 617–667–0692; FAX: 617–667–0981; E-mail: jfrangio@bidmc.harvard.edu.

this study, we have utilized optical clearing agents in these same large animal model systems of image-guided surgery, and have tried to understand the results by systematic reproduction of previously reported studies.

2 Materials and Methods

2.1 Near-Infrared Fluorescence Imaging System

The NIR fluorescence imaging system has been described in detail previously.[12] Briefly, it is composed of two wavelength-isolated excitation sources, one generating 0.5 mW/cm^2 of 400 to 650-nm white light, and the other generating 5 mW/cm^2 of 725 to 775-nm NIR excitation light, all over a 15-cm-diameter field of view (FOV). Emitted photons are collected by custom optics that separate the white light and NIR fluorescence ($>$795 nm) channels. Through computer-controlled image acquisition via LabVIEW software (Lab-VIEW, National Instruments, Austin, Texas), anatomic (white light) and functional (NIR fluorescence light) images can be displayed separately and merged. NIR fluorescence images were acquired on a 12-bit Orca-AG camera (Hamamatsu, Bridgewater, New Jersey). Color video images were acquired on an Imitech IMC-80F (Seoul, Korea) camera. All images were refreshed up to 15 times per second. The entire apparatus is suspended on an articulated arm over the surgical field at a working distance 18 in., thus permitting noninvasive and nonintrusive imaging.

2.2 Animals

Animals were used in accordance with an approved institutional protocol. Female Yorkshire pigs (E. M. Parsons and Sons, Hadley, Massachusetts) weighing 35 kg (age 11 weeks) were induced with 4.4-mg/kg intramuscular Telazol (Fort Dodge Labs, Fort Dodge, Iowa), intubated, and maintained with 1.5 to 2% isoflurane (Baxter Healthcare Corporation, Deerfield, Illinois). It should be noted that each animal had only one procedure or experiment; multiple studies were not performed on a single animal.

2.3 Perforator Vessel Near-Infrared Fluorescence Angiography

The imaging system was positioned above the ventral surface of $n=3$ animals. 10 ml of a 0.25-mg/ml (2.5 mg total; 0.092 μmol/kg) solution of indocyanine green (ICG, Sigma-Aldrich, Saint Louis, Missouri) in saline was injected via a central venous catheter as a rapid bolus. Skin perforator vessels were imaged preinjection and for 1-min postinjection at a frame rate of 500 msec and a camera exposure time of 150 msec. 100% glycerol was topically applied on a 15 $\times$15-cm area that covered the entire FOV. The glycerol was allowed to soak into the skin for 30 min. Once the fluorescence intensity in the tissue dropped to the preinjection level, another ICG injection was given, and the perforator vessels were imaged in the same manner described before. The animals were anesthetized and secured for the entire procedure to ensure a consistent sampling region between measurements. For quantitation, two images corresponding to identical vascular phases were chosen. The fluorescence intensity was quantified over two straight lines drawn over the same part of

each image. The same procedure was then performed using 50% glycerol in water and polypropylene glycol:polyethylene glycol (PPG:PEG).[14]

2.4 Near-Infrared Fluorescence Sentinel Lymph Node Mapping

ICG was preadsorbed to Cohn Fraction V bovine serum albumin (BSA, Sigma-Aldrich) at a 1:1 molar ratio,[15] and the complex (ICG:BSA) was diluted to a final concentration of 10 μM in saline. 22 groin SLN mappings were performed on $n=16$ animals by subcutaneously injecting 200 μL of ICG:BSA. The procedure was performed bilaterally in six animals. SLNs were successfully identified within 1 min in all animals. 100% glycerol, 50% glycerol in water, and PPG:PEG were topically applied 10 min after the fluorophore injection on 15$\times$15-cm areas, which covered the entire FOV. Images were obtained preinjection and 2- and 5-min postinjection, then every 5 min for 60 min after injection. In treated groups, the images were also acquired immediately following the application. Fluorescence-guided SLN resection was performed after the experiment to confirm the depth of the SLN from the skin surface. For quantitation, a circular region of interest (ROI) was drawn over the SLN and nearby background (BG) tissue. The contrast-to-background ratio (CBR) was calculated as CBR=(SLN intensity-BG intensity)/BG intensity. The percent (%) change of CBR with optimal exposure time was compared in treated and nontreated groups, with CBR set to 100% at the time of glycerol application ($T=10$ min). The animals were anesthetized and secured for the entire procedure to ensure a consistent sampling region between measurements.

2.5 Preparation and Handling of Porcine Skin for Ex-Vivo Quantitation

In 22 pigs, porcine skin was harvested from the lower part of the abdomen 4 to 8 h prior to the experiment. Subcutaneous fat was surgically removed and the skin was cut into two 9 $\times$9-cm pieces. One piece was stored in saline at 4 $^\circ$C. The other was exposed to air at both dermal and epidermal sides for between 4 and 8 h prior to the experiment. Four skin samples each from hydrated and nonhydrated harvested skin were trimmed into 2$\times$1.5-cm sections, and the thickness of each sample measured with precision calipers three times: at the sample preparation, before each measurement, and after measurement. The thicknesses of the hydrated samples were divided into three groups including 0.5, 1.0, and 1.5 mm. Eight samples were harvested from one animal. If samples deviated by more than 0.1 mm in either direction, then the samples were excluded. All nonhydrated skin samples ($n=40$) were 0.2 mm thick and were acquired from 10 animals. Hydrated skin samples with thicknesses of 0.5 mm ($n=20$), 1.0 mm ($n=30$), and 1.5 mm ($n=32$) originated from 5, 7, and 6 animals, respectively. The standard deviation of 0.2, 0.5, 1.0, and 1.5-mm-thick samples at the time of sample preparation was 0.038, 0.059, 0.053, and 0.058, respectively. 60 samples were treated with glycerol, while 62 with no treatment served as controls. The glycerol-treated group consisted of 20 nonhydrated and 40 hydrated samples, while the control group included 20 nonhydrated and 42 hydrated samples.

Table 1 Sample number in *ex-vivo* evaluation.

		Glycerol treatment		Hydration		Distance (mm)		Thickness (mm)			
		+	−	+	−	3	5	0.2	0.5	1.0	1.5
Glycerol treatment	+	NA	NA	42	20	31	31	20	10	16	16
	−	NA	NA	40	20	29	31	20	10	14	16
Hydration	+	40	42	NA	NA	40	42	0	20	30	32
	−	20	20	NA	NA	20	20	40	0	0	0
Distance (mm)	3	29	31	40	20	NA	NA	20	10	14	16
	5	31	31	42	20	NA	NA	20	10	16	16
Thickness (mm)	0.2	20	20	0	20	20	20	NA	NA	NA	NA
	0.5	10	10	20	0	10	10	NA	NA	NA	NA
	1.0	14	16	30	0	14	16	NA	NA	NA	NA
	1.5	16	16	32	0	16	16	NA	NA	NA	NA

2.6 Preparation of Near-Infrared Fluorescent Targets and Image Acquisition

NIR standards were prepared by mixing ICG:BSA with 25% gelatin at a ratio of 1:4 to produce a final ICG concentration of 10 μM. 10 μL of each NIR fluorescent standard was pipetted into equally spaced chambers in a plastic tray and allowed to harden. Excitation fluence rate was measured, and a NIR fluorescence image of the standards within the linear range of the camera was acquired. Skin samples were then sutured to wires placed at a distance of either 3 or 5 mm above the NIR standards with an air gap to recapitulate the conditions of the study by He and Wang, epidermal side up.[16] 29 of the treated and 31 of the nontreated samples were placed 3 mm over a NIR standard, while the other half of the samples, including 31 of the nonhydrated and hydrated, were placed 5 mm over a NIR standard (Table 1). Baseline images were acquired, followed immediately by application of 100% glycerol to half the samples. Samples were imaged every 10 min for 60 min after glycerol application. Skin samples were removed from the device, and the NIR standards were reimaged.

2.7 Quantitation of Fluorescence Emission Through Skin

All acquired images of NIR fluorescence emission were within the linear range of the 12-bit camera. Images were corrected for variations in excitation fluence rate and evaporation of water over the course of the experiment as follows. Obtained fluorescence intensity through each skin sample (n = 122) was divided by the corresponding fluence rate (range 2.6–5.8 mW/cm^2, mean 4.2 mW/cm^2). Due to water evaporation in the NIR fluorescent standards, the change of fluorescence intensity in NIR standards pre- and postexperiment ranged between 94 and 245% (mean 145%). Since room temperature (25 to 28 °C), air flow velocity ($\approx$0 m/s), and hu-

midity (50 to 60 %) were stable over the course of the experiment, evaporation rate (Wq) was considered constant.[17] The dye concentration at time x (min) (Cx) is relative to NIR standard volume (V):

$$Cx = 1/(V_0 − Wq^*x). \quad (1)$$

Since Wq in our experimental conditions was estimated to be <0.05 mg/min, the inverse proportional Eq. (1) could be approximated by a linear change as a function of x as x changed from 0 to 60 min.[18] Thus, estimated fluorescence intensity (E) at any time t was expressed as a function of the raw intensities of each NIR standard measured without skin pre- (I_0) and post- (I_{60}) experiment: $E(t) = (I_{60} − I_0)/60^*t + I_0$, where t is the time (min) from the start of the experiment. The fluorescence intensity of NIR standards measured through skin sample (C) was then corrected as follows: $C(t) = A(t)^*[I_0/E(t)]/F$, where $A(t)$ is the fluorescence intensity of the NIR standards imaged through skin, and F is the fluence rate measured at the individual chamber in each experiment using an Orion laser power/energy monitor and calibrated model PD300-3W photodiode (Ophir Optronics, North Andover, Massachusetts). Percentage change from baseline (PC) was defined as follows: $PC = [C(t) − C_{pretreatment}]/C^*_{pretreatment}100(\%)$.

2.8 Statistical Analysis and Histological Staining

Corrected intensity and percentage change from baseline were statistically analyzed at all data points in four categories: distance between sample and NIR standard, hydration, thickness of the sample, and glycerol treatment. A Mann-Whitney test was performed to evaluate differences in distance, hydration, and glycerol treatment with two-sided 95% confidence intervals. A Kruskal-Wallis test was used to investigate the impact of skin thickness. Multivariate analysis was subsequently per-

formed to assess the difference by condition within each group, including distance between sample and NIR standard, hydration, and thickness of the sample. Samples were divided by each condition and the impact of glycerol on corrected intensity; the percent change from baseline was compared between treated and nontreated samples. A Mann-Whitney test was used for statistical evaluation with two-sided 95% confidence intervals. All statistical evaluations were made using Prism Version 4.0 (GraphPad Software, La Jolla, California) Skin samples were histologically evaluated with hematoxylin and eosin (HE) staining after the experiment to determine if glycerol had any impact on sample morphology.

3 Results

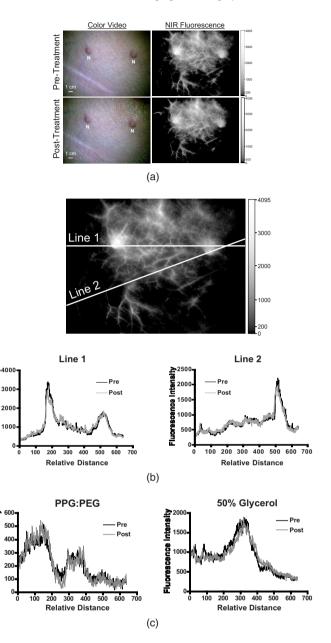### 3.1 Magnitude of the Optical Clearing Effect In Vivo

The perforator arteries and draining veins (perforator vessels) were within a few millimeters of the surface of the skin, and thus provided an ideal model system for assessing the magnitude of the optical clearing effect. Based on previously published studies, we expected a dramatic effect of glycerol on perforator vessel intensity and/or deblurring. However, as shown in Fig. 1(a), there was no qualitative difference in perforator vessel imaging using the intravenously administered NIR fluorophore ICG, even after a 30-min pretreatment with 100% glycerol, nor was there a noteworthy difference in perforator vessel intensity [Fig. 1(b)] with such treatment. The same results were obtained using 50% glycerol and PPG:PEG-treated animals [Fig. 1(c)].

Surprised by this result, we next measured the optical clearing effect during SLN mapping. As shown in Fig. 2(a), although the SLN could be identified using NIR fluorescence in all animals, application of 100% glycerol to the skin surface over the course of an hour resulted in no substantial improvement in image quality ($n = 16$). The percent change of CBR of the SLN showed no significant difference in animals that were treated or not treated with 100% glycerol ($p = 0.3263$), 50% glycerol ($p = 0.1333$), and PPG:PEG ($p = 0.1191$) [Fig. 2(b)]. Of note, the mean and standard deviation of the measured depth from the skin surface to the identified SLNs was 5.2 ± 0.075 mm.
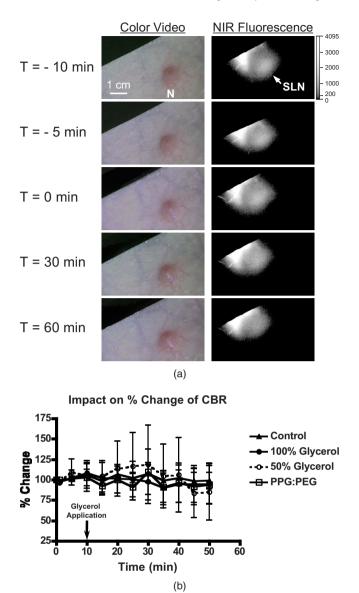
3.2 Ex-Vivo Evaluation of the Optical Clearing Effect

To understand the in-vivo results, and to reconcile previously published studies on optical clearing, we systematically evaluated the effect of skin thickness, skin hydration, distance from the skin to a fluorescent target, and glycerol treatment on NIR fluorescent target intensity. A typical experiment is shown in Fig. 3. It should be noted that all measured values were within the linear range of the 12-bit camera. However, to see all targets well in Fig. 3, contrast was enhanced such that the brightest standards appear saturated.

Quantitation of results measured for the effect of distance between skin and NIR fluorescent target, hydration, skin thickness at the time of pretreatment, and glycerol treatment (at $T = 0$, 30, and 60-min postapplication) are shown in Fig. 4(a). For all variables tested, hydration status of the skin and skin thickness consistently resulted in a statistical improvement in intensity. Distance failed to show a significant impact on corrected fluorescence. None of these three demonstrated statistical differences in terms of percentage change from

Fig. 1 The impact of optical clearing on perforator vessel NIR fluorescence angiography. (a) Intravenous injection of 0.092 μmol/kg of ICG either pretreatment (top row) or 30-min post-treatment (bottom row) of porcine skin with 100% glycerol. Shown are color video (left column) and NIR fluorescence emission (right column). NIR camera exposure time was 150 msec and normalization was identical in both sets of images. N = nipple. (b) Quantitation of fluorescence intensity, preglycerol application (black curve) and postglycerol application (gray curve), using lines (1 and 2) drawn across different vascular regions. The 12-bit intensity at each point (line plots) is shown at the bottom. (c) Quantitation of 12-bit fluorescence intensity, preapplication (black curve) and postapplication (gray curve) of PPG:PEG (left) and 50% glycerol (right).
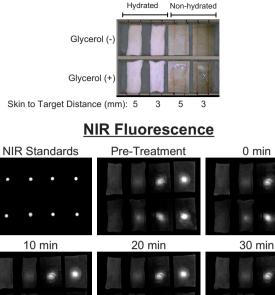
baseline (Table 2). Glycerol treatment did not show statistical improvement in either corrected intensity or percentage change from baseline over time (Table 3). When samples were stratified based on glycerol treatment [Figs. 4(b) and 4(c)], glycerol showed a statistically significant improvement in nonhydrated specimens in terms of percentage change from
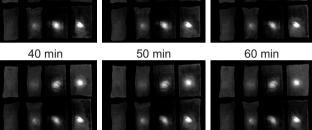
(a)

(b)

Fig. 2 Sentinel lymph node (SLN) mapping of the groin with and without glycerol treatment. (a) ICG:BSA was injected at $T=-10$ min to identify the SLN. At $T=0$, 100% glycerol was applied topically, and NIR fluorescence emission followed over the next 50 min. NIR camera exposure time was 500 msec and normalization was identical in all images. N=nipple. (b) Percent change of the CBR measured at the SLN over time in nontreated animals ($n=10$) and animals treated with 100% glycerol ($n=4$), 50% glycerol ($n=4$), and PPG:PEG ($n=4$). Point and error bar represent mean and SEM. The Mann-Whitney test showed no statistical significance between nontreated and treated groups.

baseline ($p=0.0006$) as well as corrected intensity ($p=0.0030$).

On the other hand, in the hydrated specimen, corrected intensity appeared to be better without glycerol treatment ($p=0.0011$). No statistically significant difference was seen in hydrated group in terms of percentage change from baseline [Fig. 4(b), Table 4]. Subgroup analysis of thickness revealed that glycerol treatment only had a significant impact on skin that was 0.2 mm thick, the thinnest samples of skin both in terms of intensity and change from baseline ($p=0.0030$ and
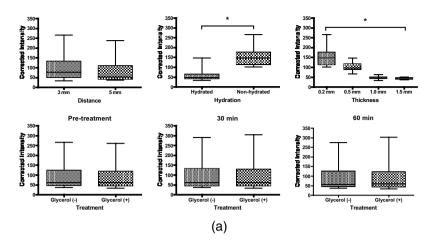

Fig. 3 Experimental setup for *ex-vivo* quantitation of the optical clearing effect in glycerol-treated porcine skin. The experimental setup described in detail in Sec. 2 is shown at top. Also shown are images of the NIR fluorescent targets before application of skin samples (NIR standards), then over time. All NIR fluorescence images were acquired with a 60-msec exposure time and were flat field corrected.
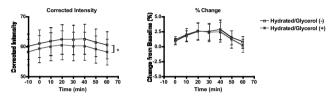
0.0006, respectively) [Fig. 4(c)]. Surprisingly, glycerol treatment showed an adverse effect in terms of intensity in the other samples with p values of 0.0030, 0.0020, and 0.0019 for 0.5, 1.0, and 1.5-mm-thick samples. There was no statistical difference in change from baseline in those samples. According to the distance between skin and NIR fluorescent target, we found glycerol treatment improved the intensity in the distance of the 3-mm group ($p=0.0070$), while no improvement was detected in the distance of the 5-mm group ($p=0.0830$). It should be mentioned that the change from baseline of the glycerol-treated group was statistically higher than that of the nontreated group in both the distances over time ($p=0.006$ and 0.0041 for 3 and 5 mm distance) (Table 4).

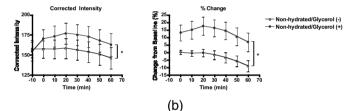### 3.3 Histological Analysis of Ex-Vivo Skin Samples

A distinctive morphological difference was observed in the SC of glycerol-treated skin samples. In hydrated skin, glycerol treatment resulted in smoothing of the SC, although no notable consistent changes were noted in the dermis or other layers of the epidermis (Fig. 5). In nonhydrated skin, glycerol treatment appeared to reduce the air gaps within the SC, and may have helped re-expand an otherwise collapsed epidermis (Fig. 5).
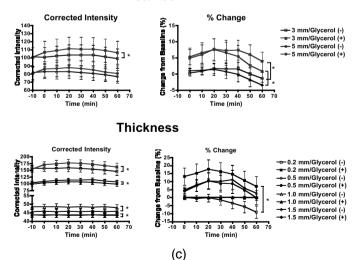
(a)

Hydrated Samples

Non-hydrated Samples

(b)

Distance

Thickness

(c)

Fig. 4 Statistical evaluation of optical clearing in *ex-vivo* specimens. (a) The impact of skin to target distance, sample hydration, skin thickness, and glycerol treatment on the corrected intensity of NIR fluorescent targets imaged through porcine skin. Asterisks indicate statistical significance. Three box plots shown in the top row represent pretreatment status. (b) Multivariate analysis by hydration status of samples. Corrected intensity and percentage change from baseline of NIR fluorescent targets imaged through hydrated (top row) or nonhydrated (bottom row) skin, with or without treatment with 100% glycerol. Point and error bar indicates mean and SEM. Asterisks indicate statistical significance. (c) Multivariate analysis by distance between sample and NIR standard (top row) and thickness of the sample (bottom row). Corrected intensity and percentage change from baseline of NIR fluorescent targets imaged with or without treatment with 100% glycerol were shown. Point and error bar indicates mean and SEM. Asterisks indicate statistical significance. Note that the corrected intensity of nontreated groups was higher than treated groups when the sample thickness was more than 0.5 mm (bottom, left).

Table 2 Impact of distance, hydration, and thickness *ex-vivo.* *Significant (glycerol treated > nontreated).

Group	p value	
	Corrected intensity	Change from baseline (%)
Distance	0.0101 to 0.1040	0.3669 to 0.7920
Hydration	<0.0001*	0.0800 to 0.9900
Thickness	<0.0001*	0.0805 to 0.7713

4 Discussion

In this study, we evaluated the potential clinical benefits of optical clearing by hyperosmotic agents during NIR fluorescence-guided surgery. We mainly focused on 100% glycerol as the clearing agent, since glycerol is an extremely common ingredient in moisturizing skin products, thus, its safety is well established for topical application to the skin. Also, glycerol was the most frequently used agent in previous studies of the optical clearing effect. Unexpectedly, our results *in vivo* showed no qualitative or quantitative advantage of glycerol treatment. To eliminate the possibility that the glycerol concentration was suboptimal for porcine skin, we repeated all of the *in-vivo* experiments using 50% glycerol in water, and obtained identical results. To explore whether these results were unique to glycerol, we repeated all of the *in-vivo* experiments using topical application of a mixture of PPG:PEG.[14] Once again, there was no qualitative or quantitative effect of the agent.
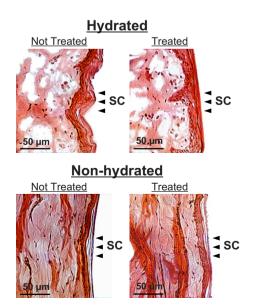
However, subsequent *ex-vivo* experiments revealed an advantage for nonhydrated and thin samples, the changes of which were only statistically significant in corrected intensity. The *ex-vivo* optical clearing effect of glycerol has two possible mechanisms. One is an optical effect due to refractive index matching, which would appear immediately after the application. The second is mechanical alteration of the skin,

Table 3 Statistical evaluation of optical clearing effects of glycerol *ex-vivo.*

Time (min)	p value	
	Corrected intensity	Change from baseline (%)
Pretreatment	0.7626	—
0	0.9694	0.1190
10	0.9286	0.1960
20	0.9002	0.1676
30	0.8921	0.2087
40	0.8799	0.0786
50	0.9816	0.1178
60	0.8921	0.1568

Table 4 Multivariate analysis of clearing impact of the glycerol *ex-vivo.* *Significant (glycerol treated > nontreated). **Significant (glycerol treated < nontreated).

Group	Subgroup	p value	
		Corrected intensity	Change from baseline (%)
Distance	3 mm	0.0070*	0.0060*
Distance	5 mm	0.0830	0.0040*
Hydration	–	0.0030*	0.0006*
Hydration	+	0.0011**	0.8048
Thickness	0.2 mm	0.0030*	0.0006*
Thickness	0.5 mm	0.0030**	0.8048
Thickness	1.0 mm	0.0002**	0.5350
Thickness	1.5 mm	0.0019**	1.0000

which could continue to change over time. Corrected intensity primarily reflected the refractive index effect, while change from baseline represented mechanical changes. Our results suggest that both effects can occur *ex vivo*. When samples were stratified in more detail, we found that glycerol did have a significant optical clearing effect on both corrected intensity and change from baseline in limited situations, such as nonhydrated, thin skin samples (i.e., 0.2-mm-thick samples), and close distance (i.e., 3 mm) to the targeted object. Indeed, the histological effect of glycerol was only seen at the SC, and possibly the outermost epidermis. A significant improvement in fluorescence imaging generally requires enhancement of both the penetration of excitation light into tissue, and the

Fig. 5 *Ex-vivo* histological analysis of skin samples. HE staining of hydrated (top row) and nonhydrated (bottom row) skin samples either not treated (left column) or treated (right column) with 100% glycerol. SC = stratum corneum.

escape of emitted light from tissue. The lack of effect of optical clearing agents *in vivo* is likely explained by relative contribution of SC to optical path length. As shown in Fig. 5, the thickness of the SC was $\approx 2-10\ \mu$m in nonhydrated skin and $\approx 4-20\ \mu$m in hydrated skin. This is equivalent to ≈ 1 to 5% of the path length in 0.2-mm-thick samples (i.e., nonhydrated samples), and 0.8 to 4%, 0.4 to 2%, and 0.2 to 1.3% of the path length in 0.5, 1.0 and 1.5-mm-thick samples (i.e., hydrated samples), respectively. A previous study, in fact, verified that the SC layer has no significant effect on the refractive index of skin.[19] Furthermore, particles that contribute most to light scatter in living tissue are subsurface, cellular components. Mourant et al.[20] found that nuclei are responsible for 40% of scattering in whole cells, while Beauvoit, Kitai, and Chance[21] suggested that mitochondria were the predominant source of light scattering in the liver. In our *ex-vivo* experiments, the optical clearing effect was shown statistically to be limited to nonhydrated skin samples, and were most pronounced in the 0.2-mm-thick samples, which is consistent with a localized effect.

Recently, several studies showed the potential benefit of using hyperosmotic agents in phototherapy. Vargas, Barton, and Welch[22] demonstrated that pretreatment of the skin with 50% glycerol reduced the radiant exposure of the laser required for vessel photocoagulation. Also, Khan et al.[14] reported that less skin damage from laser exposure was found both clinically and histologically by topical application of PPG:PEG. In their study, they used a YAG laser to excise skin samples with and without pretreatment of PPG:PEG, and reported a decrease in basal cell vacuolization and separation at the dermoepidermal junction (DEJ) in pretreated skin. They also concluded that erythema and blisters were less frequently found in PPG:PEG pretreated areas after laser treatment for tattoo removal. We investigated the optical clearing effect of PPG:PEG in NIR fluorescence angiography *in vivo* using the same treatment with PPG:PEG, and saw no enhancement with PPG:PEG [Fig. 1(c)]. A possible explanation is that skin damage at the DEJ may be diminished by hyperosmotic agents acting on the SC, which in turn reduces scatter in the epidermis. In other words, the impact on the SC is significant at least in terms of delivery of light to the DEJ. Targeting the superficial layer of the skin with phototherapy may indeed be more effective and safer with pretreatment using hyperosmotic agents; however, this effect does not translate into a benefit for NIR fluorescence image-guided surgery, even when relatively superficial targets, such as perforator vessels, are imaged, because the effect was not considered significant enough to enhance the return of emitted light.

Topically applied hyperosmotic agents have been used as optical clearing materials in previous studies utilizing both optical coherence tomography (OCT)[2,23–25] and low-level emitted light (bioluminescence) imaging.[16] Although it is possible that OCT may be more sensitive to alterations of light penetration induced by glycerol than NIR imaging, it is also possible that dehydration from air exposure during the procedure is creating a situation analogous to our nonhydrated *ex-vivo* samples, and that glycerol is acting to change the hydration status of the tissue.[2,4,6,26] The previously reported bioluminescence experiments utilized an extremely weak light source, which required exposure times as long as 60 sec for

quantitation,[16] and skin to target air gap distances of 3 and 5 mm. More importantly, the description of this study suggests that the skin samples were nonhydrated prior to, and during, imaging.

To enhance the transepidermal delivery of hyperosmotic agents, removal of the SC using sandpaper[27] or tape stripping[28] has been attempted. Though this procedure undoubtedly causes inflammation, it could still be used in research-based or limited clinical applications, such as phototherapy, where the benefit may outweigh the adverse effects on the skin. Other previously published studies that employed dermal side or subcutaneous application suggested that the potential optical clearing effect of hyperosmotic agents could be dramatic if the barrier function of the SC were eliminated.[6,11,26] Similarly, application of hyperosmotic agents on digestive tract mucosa, which lack an SC entirely, may produce improved imaging depth and contrast for diagnosis.[29,30] However, the optical clearing effects of such agents on the digestive tract were only studied *ex vivo* using OCT, therefore safety and utility must be established *in vivo* before conclusions can be drawn.

In summary, hyperosmotic agents such as glycerol and PPG:PEG may produce a significant optical clearing effect under highly manipulated model systems, but during NIR fluorescence image-guided surgery of well-vascularized, well-hydrated tissue, there appears to be no qualitative or quantitative effect of these agents.

References

1. J. V. Frangioni, "In vivo near-infrared fluorescence imaging," *Curr. Opin. Chem. Biol.* **7**, 626–634 (2003).
2. R. K. Wang, V. V. Tuchin, and J. B. Elder, "Concurrent enhancement of imaging depth and contrast for optical coherence tomography byy hyperosmotic agents," *J. Opt. Soc. Am. B* **18**, 948–953 (2001).
3. S. Plotonikov, V. Juneja, A. B. Isaacson, W. A. Mohler, and P. J. Campagnola, "Optical clearing for improved contrast in second harmonic generation imaging of skeletal muscle," *Biophys. J.* **90**, 328–339 (2006).
4. Y. He and R. K. Wang, "Dynamic optical clearing effect of tissue impregnated with hyperosmotic agents and studied with optical coherence tomography," *J. Biomed. Opt.* **9**, 200–206 (2004).
5. H. Cheng, Q. Luo, S. Zeng, S. Chen, W. Luo, and H. Gong, "Hyperosmotic chemical agent's effect on in vivo cerebral blood flow revealed by laser speckle," *Appl. Opt.* **43**, 5772–5777 (2004).
6. G. Vargas, K. F. Chan, S. L. Thomsen, and A. J. Welch, "Use of osmotically active agents to alter optical properties of tissue: effects on the detected fluorescence signal measured through skin," *Lasers Surg. Med.* **29**, 213–220 (2001).
7. A. T. Yeh, B. Choi, J. S. Nelson, and B. J. Tromberg, "Reversible dissociation of collagen in tissues," *J. Invest. Dermatol.* **121**, 1332–1335 (2003).
8. J. Hirshburg, B. Choi, J. S. Nelson, and A. T. Yeh, "Collagen solubility correlates with skin optical clearing," *J. Biomed. Opt.* **11**, 040501 (2006).
9. B. Choi, L. Tsu, E. Chen, T. S. Ishak, S. M. Iskandar, S. Chess, and J. S. Nelson, "Determination of chemical agent optical clearing potential using in vitro human skin," *Lasers Surg. Med.* **36**, 72–75 (2005).

10. G. Vargas, A. Readinger, S. S. Dozier, and A. J. Welch, "Morphological changes in blood vessels produced by hyperosmotic agents and measured by optical coherence tomography," *Photochem. Photobiol.* **77**, 541–549 (2003).

11. E. D. Jansen, P. M. Pickett, M. A. Mackanos, and J. Virostko, "Effect of optical tissue clearing on spatial resolution and sensitivity of bioluminescence imaging," *J. Biomed. Opt.* **11**, 041119 (2006).

12. E. Tanaka, H. S. Choi, H. Fujii, M. G. Bawendi, and J. V. Frangioni, "Image-guided oncologic surgery using invisible light: completed pre-clinical development for sentinel lymph node mapping," *Ann. Surg. Oncol.* **13**, 1671–1681 (2006).

13. A. Matsui, B. T. Lee, J. Winer, C. S. Vooght, and J. V. Frangioni, "Real-time intraoperative near-infrared fluorescence angiography for perforator identification and flap design," *Plast. Reconstr. Surg.* (in press).

14. M. H. Khan, S. Chess, B. Choi, K. M. Kelly, and J. S. Nelson, "Can topically applied optical clearing agents increase the epidermal damage threshold and enhance therapeutic efficacy?" *Lasers Surg. Med.* **35**, 93–95 (2004).

15. S. Ohnishi, S. J. Lomnes, R. G. Laurence, A. Gogbashian, G. Mariani, and J. V. Frangioni, "Organic alternatives to quantum dots for intraoperative near-infrared fluorescent sentinel lymph node mapping," *Mol. Imaging* **4**, 172–181 (2005).

16. Y. He and R. K. Wang, "Improvement of low-level light imaging performance using optical clearing method," *Biosens. Bioelectron.* **20**, 460–467 (2004).

17. M. W. Zemansky and R. H. Dittman, *Heat and Thermodynamics: An Intermediate Textbook*, 6th ed., pp. 265–266 (1981).

18. K. Hisatake, S. Tanaka, and Y. Aizawa, "Evaporation rate of water in a vessel," *J. Appl. Phys.* **73**, 7395–7401 (1993).

19. H. Ding, J. Q. Lu, W. A. Wooden, P. J. Kragel, and X. H. Hu, "Refractive indices of human skin tissues at eight wavelengths and estimated dispersion relations between 300 and 1600 nm," *Phys. Med. Biol.* **51**, 1479–1489 (2006).

20. J. R. Mourant, M. Canpolat, C. Brocker, O. Esponda-Ramos, T. M. Johnson, A. Matanock, K. Stetter, and J. P. Freyer, "Light scattering from cells: the contribution of the nucleus and the effects of proliferative status," *J. Biomed. Opt.* **5**, 131–137 (2000).

21. B. Beauvoit, T. Kitai, and B. Chance, "Contribution of the mitochondrial compartment to the optical properties of the rat liver: a theoretical and practical approach," *Biophys. J.* **67**, 2501–2510 (1994).

22. G. Vargas, J. K. Barton, and A. J. Welch, "Use of hyperosmotic chemical agent to improve the laser treatment of cutaneous vascular lesions," *J. Biomed. Opt.* **13**, 021114 (2008).

23. M. Oldham, H. Sakhalkar, T. Oliver, G. Allan Johnson, and M. Dewhirst, "Optical clearing of unsectioned specimens for three-dimensional imaging via optical transmission and emission tomography," *J. Biomed. Opt.* **13**, 021113 (2008).

24. O. F. Stumpp, A. J. Welch, T. E. Milner, and J. Neev, "Enhancement of transepidermal skin clearing agent delivery using a 980 nm diode laser," *Lasers Surg. Med.* **37**, 278–285 (2005).

25. G. Vargas, E. K. Chan, J. K. Barton, H. G. Rylander, 3rd, and A. J. Welch, "Use of an agent to reduce scattering in skin," *Lasers Surg. Med.* **24**, 133–141 (1999).

26. C. G. Rylander, O. F. Stumpp, T. E. Milner, N. J. Kemp, J. M. Mendenhall, K. R. Diller, and A. J. Welch, "Dehydration mechanism of optical clearing in tissue," *J. Biomed. Opt.* **11**, 041117 (2006).

27. O. Stumpp, B. Chen, and A. J. Welch, "Using sandpaper for noninvasive transepidermal optical skin clearing agent delivery," *J. Biomed. Opt.* **11**, 041118 (2006).

28. R. J. McNichols, M. A. Fox, A. Gowda, S. Tuya, B. Bell, and M. Motamedi, "Temporary dermal scatter reduction: quantitative assessment and implications for improved laser tattoo removal," *Lasers Surg. Med.* **36**, 289–296 (2005).

29. X. Xu and R. K. Wang, "Synergistic effect of hyperosmotic agents of dimethyl sulfoxide and glycerol on optical clearing of gastric tissue studied with near infrared spectroscopy," *Phys. Med. Biol.* **49**, 457–468 (2004).

30. R. K. Wang and J. B. Elder, "Propylene glycol as a contrasting agent for optical coherence tomography to image gastrointestinal tissues," *Lasers Surg. Med.* **30**, 201–208 (2002).